JOURNAL OF MATERIALS SCIENCE **36** (2001) 2645 – 2650

The effect of contour angle on fractal dimension measurements for brittle materials

A. DELLA BONA, T. J. HILL, J. J. MECHOLSKY*, JR.
Departments of Material Sciences and Engineering and Dental Biomaterials, University of Florida, Gainesville, FL, 32611, USA
E-mail: jmech@mse.ufl.edu

Slit-island analysis (SIA) has been successfully used to measure the fractal dimensional increment (D^*) of fracture surfaces. The fracture toughness in brittle ceramics is related to the fractal dimension. However, the measurement technique may affect the determined D^* values. The purpose of this study was to determine the contour angle at which a valid fractal dimension measurement could be obtained using the SIA method for baria silicate glass-ceramic and zinc selenide ceramic. Two specimens of each material were duplicated for each of the following contour angles: 0°, 3°, 5°, 7°, 22°, and 90°. After polishing to 1 μm alumina slurry, the coastlines were photographed and arranged in a collage. The coastline was analyzed using the Richardson technique. Results showed that the SIA technique is sensitive to the contour angle since D^* decreases with increasing contour angle for both materials.

1. Introduction

The use of fractal dimension measurements to characterize rough surfaces, *e.g.* fracture surfaces, has become popular since Mandelbrot (1982) [1] re-introduced the concept of fractal geometry. Fractals are geometrical objects that permit fractional dimensions. Several authors have used fractal geometry to quantitatively describe irregular fracture surfaces [2–11]. Thus, a fracture surface may have the fractal dimension of, say, 2.3 where 2 is the topological dimension and 0.3 is the fractal dimensional increment, D^*. Fractography has been used to quantitatively relate the stress at failure, the nature of the stress state and the amount of residual stress to the sizes of the initial crack and surrounding topography [12]. Fractography also has been used to relate the flaw/mirror size ratio and the fracture toughness, which, in turn, is related to the elastic modulus. The combination of these relationships show that the fractal dimensional increment, D^*, is directly related to the flaw/mirror size ratio. This implies that there is a linear scaling law between the energy of crack initiation and the energy of microbranching at fracture and this relationship is reflected in the features on the fracture surface [12, 13].

The conceptual simplicity of the fractal dimension for a surface is not matched by ease of measurement. Many researchers [2, 7, 8, 10, 11, 14–16] have used slit-island analysis (SIA) to obtain fracture surface (horizontal) contours, along with the Richardson technique for fractal dimension determination. Some of Mandelbrot's original conjectures [1, 2] about (1) surfaces and cuts through them, (2) projections of fractal structures onto a low-dimensional surface, and (3) isotropy of surfaces, are not necessarily applicable to experimental measurements [17].

It is also necessary to differentiate self-similarity, in which the dimensions in the z direction scale in the same way as those in x and y, from self-affinity in which they do not [16]. Many fracture surfaces are most likely self-affine rather than self-similar [18]. Thus, the basic idea that fracture surfaces are self-affine, and self-similar in the horizontal plane, means that detailed structure is still observed at progressively finer dimensions [16]. However, this may not be true once the measurements are made out of the horizontal plane of fracture. Therefore, the objective of this study is to determine the contour angle at which a valid fractal dimension measurement can be obtained using the SIA method for baria silicate glass-ceramic ($3BaO{\cdot}5SiO_2$) and zinc selenide ceramic (ZnSe).

2. Materials and methods

Materials with different microstructures were selected to study the effect of contour angle on fractal dimension measurements. A baria silicate glass-ceramic with a large crystal aspect ratio and small grains (~3–10 μm), and a zinc selenide polycrystalline ceramic with large grains (~50–100 μm), were used in this study. The microstructure and mechanical properties of these materials were previously studied and reported [19, 20].

All fracture surfaces were produced from specimens loaded in 4-point flexure to failure. Two specimens of each material were studied, and each contour or

* Author to whom all correspondence should be addressed.

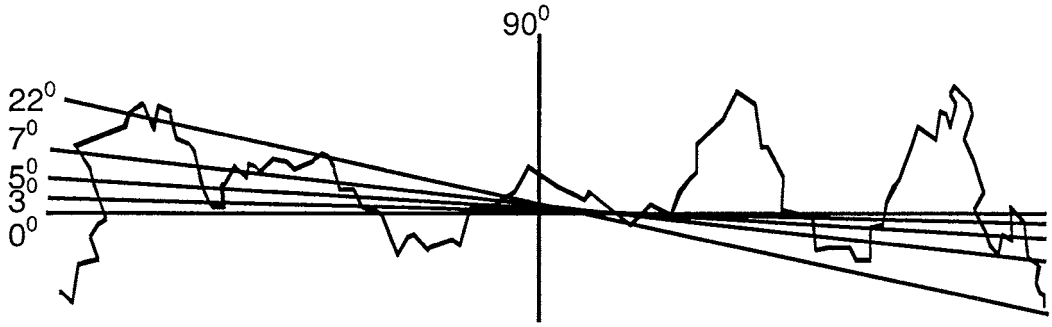

Figure 1 Schematic representation of a fracture surface profile and the contour angles used in this study.

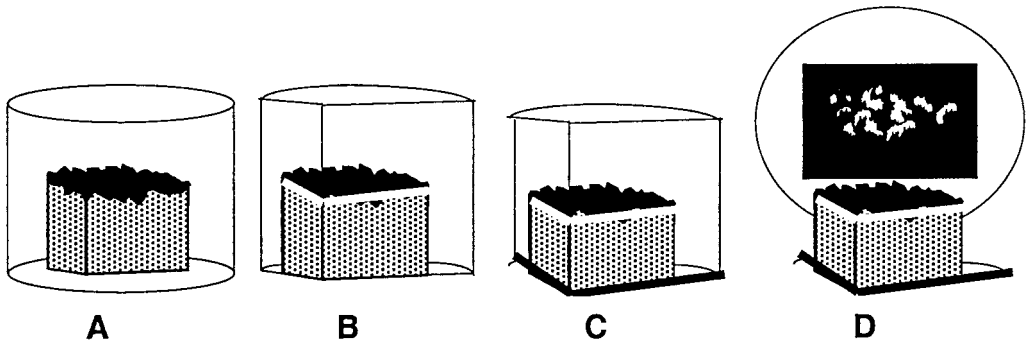

Figure 2 Schematic representation of the sequence of procedures to obtain the contour angle images for the modified slit-island analysis.

polishing angle (0, 3, 5, 7, 22, and 90 degrees), as shown in Fig. 1, was created on the exact same specimen by using a replication technique detailed in a companion paper [16]. Previous research [7, 19, 21] showed that typical standard deviations in fractal dimension measurements were 0.01 to 0.03. Therefore, six epoxy resin replicas of each fracture surface were made for a total of 24 specimens. All the specimens were sputter-coated with gold-palladium for 4 min in a Hummer II Sputter Coater (21020, Technics Inc., Alexandria, VA, USA) at a current of 10 mAmp, and vacuum of 130 mTorr to produce a thick high contrast layer. A layer of epoxy resin was poured over the coated replica to form a sandwich-type structure of epoxy/coating/epoxy (Fig. 2A). Except for the 90° contour angle specimens, three slices, forming a triangle on the outside of the epoxy replica, were made and polished, so that the fracture plane could be visualized and marked (white line in Fig. 2B). Specimens were mounted, upside down, in a fast set gypsum stone with the marked fracture surface leveling the top of the stainless steel holder. After the stone had set, the holder containing the specimen was magnetically fixed to the platform of a precision milling machine (CM Dental, Cendres & Metaux SA, CH-2501, Biel-Bienne) that was adjusted to the desired cutting angle. Care was taken to allow the horizontal cut to start on the same side as the fracture initiated in the up-side-down surface specimen. Once the bottom of the specimens were cut flat to the desired angles (black line in Fig. 2C), they were taken out of the stone and mounted up-right on polishing lappers. For the 90° contour angle, the specimens were cut perpendicular to the fracture surface and mounted on polishing lappers. All specimens were ground down until "islands" appeared on the fracture surface, and polished to 1 μm alumina slurry (Fig. 2D).

TABLE I Polishing or contour angles and fractal dimensional increment, D^*, for baria silicate glass-ceramic and zinc selenide ceramic. (n1) and (n2) represent the two measurements obtained for each sample

Contour Angle	D^* (Baria Silicate) (n1); (n2): **Average**	D^* (Zinc Selenide) (n1); (n2): **Average**
0°	(0.31); (0.26): **0.28**	(0.13); (0.12): **0.13**
3°	(0.24); (0.23): **0.23**	(0.11); (0.10): **0.11**
5°	(0.20); (0.21): **0.21**	(0.08); (0.08): **0.08**
7°	(0.17); (0.17): **0.17**	(0.03); (0.04): **0.03**
22°	(0.14); (0.15): **0.15**	(0.03); (0.03): **0.03**
90°	(0.03); (0.02): **0.03**	(0.03); (0.01): **0.02**

For the modified slit-island analysis, a series of 8–10 photographs were taken of the coastline, at a magnification of 400×. The photographs were arranged in a collage (Fig. 3) where the coastline was measured using the Richardson technique, as described in a companion paper [16].

3. Results

The fractal dimensional increment, D^*, obtained for the six contour angles for baria silicate glass-ceramic and zinc selenide ceramic are presented in Table I. The data are also graphed in Figs 4 and 5. A representative image of the fracture surface of each contour angle for baria silicate glass-ceramic and zinc selenide ceramic are, respectively, presented in Fig. 6 and Fig. 7. Many measurements have been made on the fractal dimensional increment (D^*) on $3BaO{\cdot}5SiO_2$ and ZnSe as well as other materials in previous work [7, 16, 19, 20, 21]. Typical D^* values, when using the SIA technique, have a standard deviation ranging from ± 0.01 to ± 0.03, which is in the range reported in this study. It is apparent that the slit-island technique is very sensitive to contour angle for both the baria silicate glass-ceramic

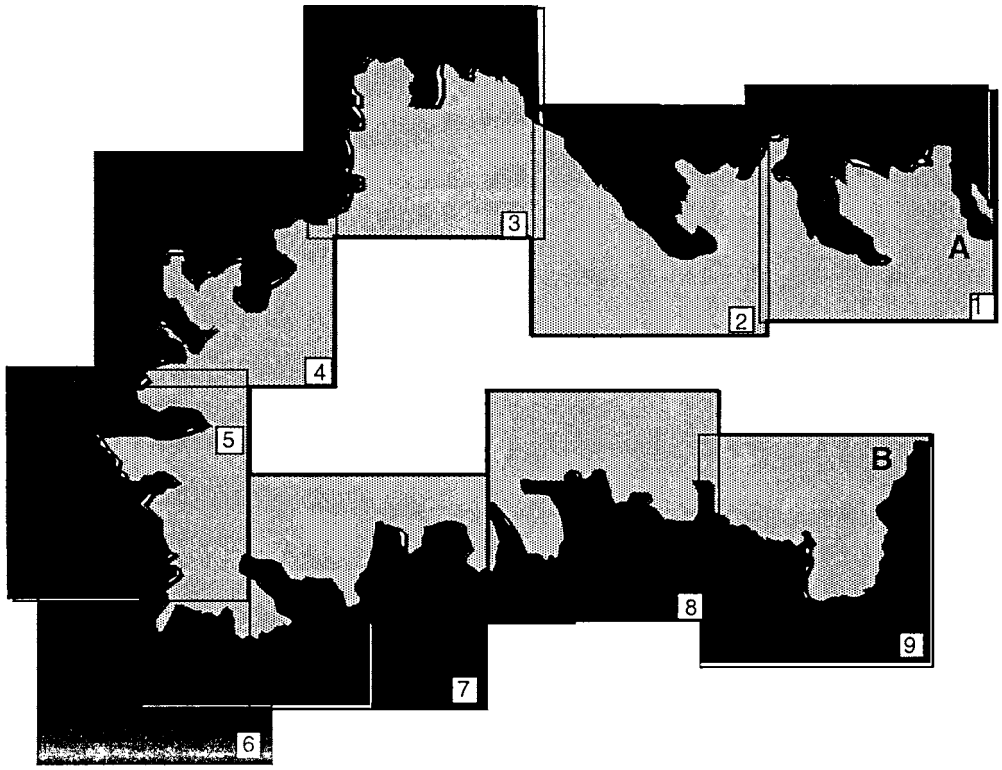

Figure 3 Schematic of a collage made of 9 photographs. The length of coastline should be measured from point A to B using dividers of varying sizes (Richardson technique).

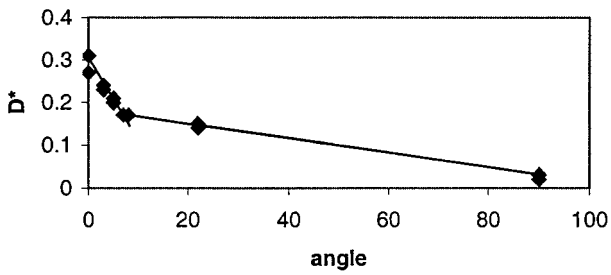

Figure 4 Fractal dimensional increment (D^*) values with respect to contour angles for baria silicate glass-ceramic.

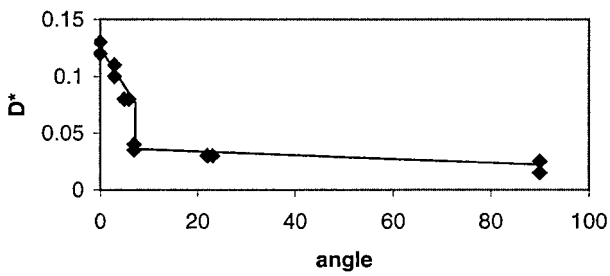

Figure 5 Fractal dimensional increment, D^*, values with respect to contour angles for zinc selenide ceramic.

and the zinc selenide ceramic. The boundaries produced by the different contour angles showed different levels of tortuosity corresponding to the measurements shown in Table I.

At a zero degree angle (parallel to the fracture surface), the size of the polished islands is much larger for the zinc selenide ceramic than for the baria silicate. This difference can be due to either a different depth of cut for tortuous materials, or due to different grain sizes or microstructural features for the same depth of cut. If the difference is due to different depth of cuts, then the coastline measurements should result in the same fractal dimension values, which they do not for the same material. In the case for the same depth of cut, a large grained material will produce what appear to be fewer, large islands, due to the distance between boundaries, and the small grained material will produce many, smaller islands. Since there is a large difference in microstructural features between the $3BaO{\cdot}5SiO_2$ ($\sim$3–10 μm) and ZnSe ($\sim$10–100 μm), the most likely reason for the difference in size of islands, for the many different depth of cuts that were made, is primarily the difference in microstructural features.

At the 5° angle and below, islands appear for both materials. For angles greater than 5°, only isolated contour lines appear (Figs 6 and 7). This observation becomes very evident when the profile technique [16] is used to obtain the coastline for the 90° contour angle (Figs 6 and 7, 90°). For angles greater than 5°, the polishing or contour plane starts missing all neighboring texture. The images from Figs 6 and 7 correlate with the data shown in Table I and graphed in Figs 4 and 5. These data show that there is a large change in D^* values for angles greater than 5°.

The D^* values obtained from the 5° and below contour angle data for the baria silicate glass-ceramic and zinc selenide ceramic are in agreement with the predicted lines on the $D^{*1/2}$ versus K_{IC} graph for the modified SIA values (Fig. 8) presented in other studies [16, 19].

4. Discussion

Experimental procedures to obtain slit islands to measure D^* involve polishing a fracture surface. Since one cannot precisely know either the polishing altitude or the orientation of the polishing plane, it is important

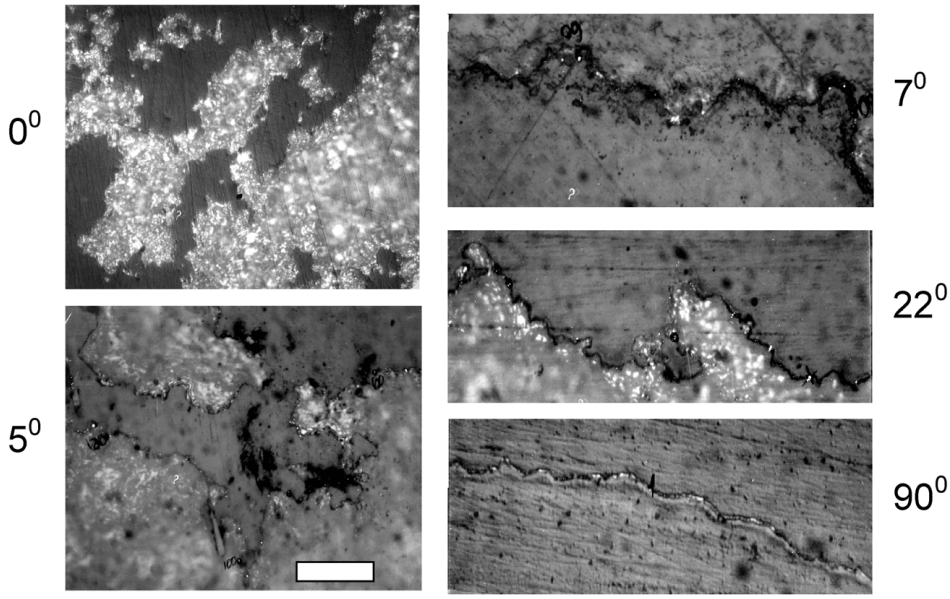

Figure 6 Coastline images for baria silicate glass-ceramic. Increase in contour angle shows corresponding decrease in roughness (magnification 400×). [Bar = 25 microns for all angles.]

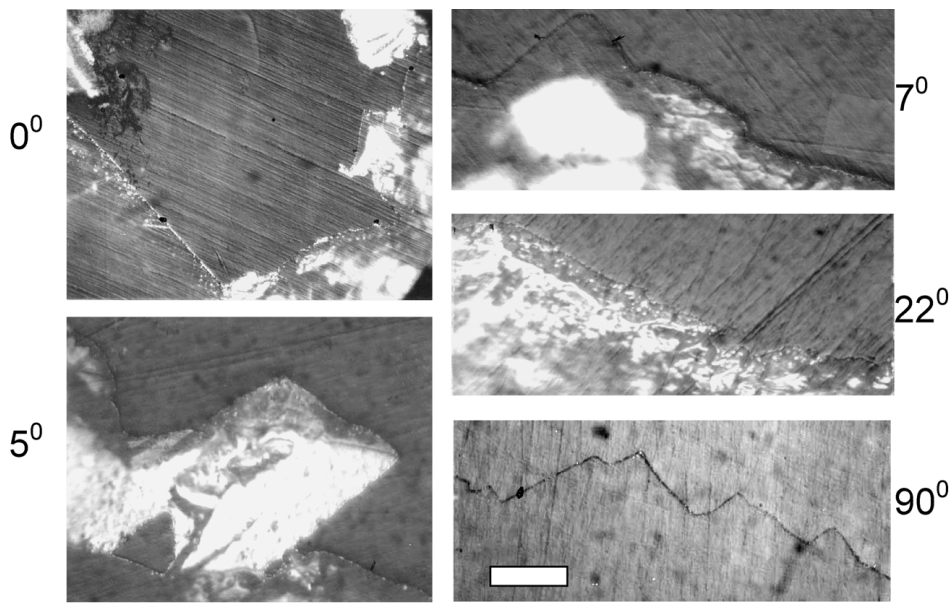

Figure 7 Coastline images for zinc selenide ceramic. Increase in contour angle shows corresponding decrease in roughness (magnification 400×). [Bar = 25 microns for all angles.]

to understand how contour dimension may vary with polishing or contour angle and altitude.

This study has shown that a slight variation of over 5° on the polishing angle produces significant variation on the appearance of the coastline (Figs 6 and 7) that, consequently, affects the values obtained for D^*. At the 5° angle and smaller, islands appear for both materials. A higher density number of islands are clearly observed in a single micrograph for baria silicate glass-ceramic than for zinc selenide ceramic. This can be explained by the difference in grain size between the two materials, in which the smaller grained, large crystal aspect ratio material would produce smaller islands located in closer proximity to each other than a large grained material, like zinc selenide. Thus, there is not a change in measurement principle between the two materials, only a change in scale.

For angles equal to or greater than 7°, only isolated contour lines appear (Figs 6 and 7). These single contour lines, as opposed to the complete islands, show a different degree of tortuosity or roughness for each material. For the $3BaO{\cdot}5SiO_2$ glass ceramic, the closed islands [≤5°] have D^* values >0.2 and the isolated lines have D^* values below 0.2. For ZnSe, the values for D^* drop below 0.08 [at 5°] to 0.03 [at 7°] corresponding to the change from closed islands to single contour lines. This suggests that the degree of tortuosity is dependent on the size of the microstructure on the fracture surface and the degree of divergence from the fracture plane. After the 7° angle, the polishing or contour plane starts missing all neighboring texture, and at 90° it does not retain any significant feature of the fracture surface but a profile representation of the surface roughness. Note that this demonstrates that a single profile does

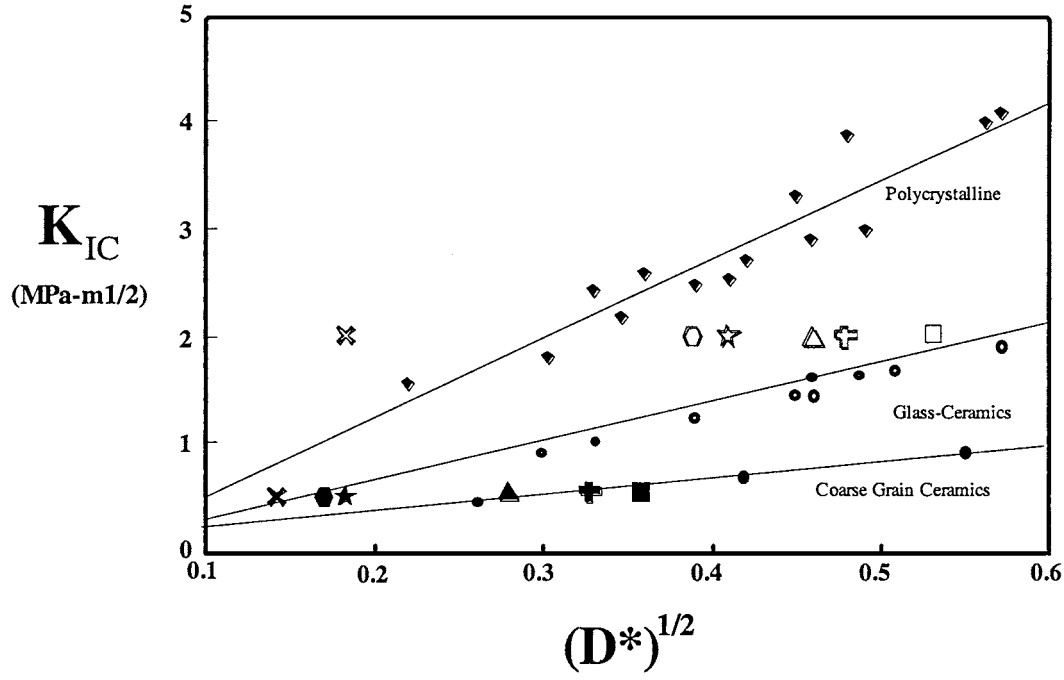

Figure 8 Fracture toughness versus fractal dimensional increment for material classes including materials and contour angles used in this study. Squares −0°; Greek crosses −3°; triangles −5°; stars −7°; hexagons −22°; Saint Andrew's crosses −90°. Open symbols are for baria silicate glass-ceramic, and filled symbols are for zinc selenide ceramic.

not represent the texture of the fracture surface for self-affine fractals.

The contour dimension change with polishing angle effect is in agreement with a study by Mackin [21] who investigated the fractal dimension using computer modeled fracture surfaces. He showed that there was no significant difference in contour dimension with altitude, and that the roughness parameter (H) is related to surface dimension ($\Delta z = \Delta t^H$, where Δz is the change in vertical scale and Δt is the change in horizontal scale). For self-similar fractal structures, $H = 2 - D$ for surfaces. However, this relationship does not hold for self-affine structures [17], such as fracture surfaces. As H increases the surface texture diminishes and the surface dimension decreases. Mackin also concluded that there was no apparent relationship between the surface (horizontal plane) and profile (vertical plane) dimensions. Mandelbrot [22] and Russ [17] also stated that profile dimension has no relationship to surface dimension for self-affine surfaces. However, this relationship holds for self-similar surfaces. Recall that fracture surfaces of materials that fail in a brittle manner are most likely self-affine, but are self-similar in an horizontal plane.

5. Conclusions

The results of this study showed: (1) the measured fractal dimensional increment, D^*, decreases with increasing contour angle for the baria-silicate glass-ceramic and zinc selenide ceramic; (2) the D^* values obtained using the SIA technique are very sensitive to the contour angle; and (3) D^* values vary with fracture surface structure following the predicted material class lines on the K_{IC} versus $D^{*1/2}$ graph.

Future research should focus on modeling real fracture surfaces, and use other imaging techniques, such as atomic force microscopy, to verify at all scales the observations made in this study.

Acknowledgments

Supported by CAPES do Brazil, and NIH/NIDCR Grant Nos. DE09307 and DE06672. The authors thank Professor Thomas J. Mackin of the University of Illinois for useful discussions.

References

1. B. B. MANDELBROT, in "The Fractal Geometry of Nature" (W. H. Freeman & Co., San Francisco, 1982).
2. B. B. MANDELBROT, D. E. PASSOJA and A. J. PAULLEY, *Nature* **308** (1984) 721.
3. J. J. MECHOLSKY JR., D. E. PASSOJA and K. S. FEINBERG-RINGEL, *J. Amer. Ceram. Soc.* **72** (1989) 60.
4. D. J. ALEXANDER, in "Quantitative Methods in Fractography" (ASTM STP 1085, Philadelphia, 1990) p. 39.
5. G. PEZZOTTI, M. SAKAI, Y. OKAMOTO and T. NISHIDA, *Mater. Sci. Eng.* **A197** (1995) 109.
6. J. WASEN, E. HEIER and T. HANSSON, *Scripta Materialia* **38**(6) (1998) 953.
7. J. J. MECHOLSKY JR. and J. R. PLAIA, *J. Non-Cryst. Solids* **146** (1992) 249.
8. Z. CHEN, J. J. MECHOLSKY JR., T. JOSEPH and C. L. BEATTY, *J. Mater. Sci.* **32** (1997) 6317.
9. J. C. HSIUNG and Y. T. CHOU, *ibid.* **33** (1998) 2949.
10. C. S. PANDE, L. E. RICHARDS, N. LOUAT, B. D. DEMPSEY and A. J. SCHWOEBLE, *Acta Metall.* **35**(7) (1987) 1633.
11. C. S. PANDE, L. E. RICHARDS and S. SMITH, J. *Mater. Sci. Let.* **6** (1987) 295.
12. J. J. MECHOLSKY JR., in "Fractography of Glasses and Ceramics III," edited by J. R. Varner, V. D. Frechette and G. D. Quinn (Ceramic Transactions, Vol. 64, 1996) p 385.
13. J. J. MECHOLSKY JR. and S. W. FREIMAN, *J. Amer. Ceram. Soc.* **74**(12) (1991) 3136.
14. C. W. LUNG, in "Fractals in Physics" (North Holland, Amsterdam, 1985) p. 189.
15. C. W. LUNG and Z. Q. MU. *Phys. Rev.* **B38** (1988) 11781.

16. T. J. HILL, A. DELLA BONA and J. J. MECHOLSKY JR., *J. Mater. Sci*. **36** (2001) 2651.
17. J. C. RUSS, in "Fractal Surfaces" (Plenum Press, New York, 1994).
18. *Idem*. J. Computer-Assisted Microscopy, **3**(3) (1991) 127.
19. T. J. HILL, J. J. MECHOLSKY JR. and K. J. ANUSAVICE, *J. Amer. Ceram. Soc*. **83**(3) (2000) 545.
20. S. W. FREIMAN, J. J. MECHOLSKY JR., R. W. RICE and J. C. WURST, *ibid*. **58**(9/10) (1975) 406.
21. T. J. MACKIN, Ph.D. Thesis, Penn State University, 1990.
22. B. B. MANDELBROT, *Physica Scripta* **32** (1985) 257.

Received 20 June
and accepted 27 November 2000